European Journal of Pharmaceutics and Biopharmaceutics 79 (2011) 102–107

Contents lists available at ScienceDirect

European Journal of Pharmaceutics and Biopharmaceutics

journal homepage: www.elsevier.com/locate/ejpb

Research paper

Preparation and characterization of triclosan nanoparticles intended to be used for the treatment of acne

Clara Luisa Domínguez-Delgado, Isabel Marlen Rodríguez-Cruz, José Juan Escobar-Chávez, Iván Omar Calderón-Lojero, David Quintanar-Guerrero, Adriana Ganem *

División de Estudios de Posgrado (Laboratorio de Posgrado en Tecnología Farmacéutica), Facultad de Estudios Superiores Cuautitlán, Estado de México, Mexico

ARTICLE INFO

Article history:
Received 22 October 2010
Accepted in revised form 26 January 2011
Available online 2 February 2011

Keywords:
Skin
Acne
Triclosan
Nanoparticles
Emulsion
Percutaneous permeation

ABSTRACT

This work focuses on the preparation and characterization of nanoparticles containing triclosan. Additionally, *in vitro* percutaneous permeation of triclosan through pig ear skin was performed, and comparisons were made with two commercial formulations: An o/w emulsion and a solution, intended for the treatment of acne. The nanoparticle suspensions were prepared by the emulsification–diffusion by solvent displacement method, using Eudragit® E 100 as polymer. All batches showed a size smaller than 300 nm and a positive Zeta potential, high enough (20–40 mV) to ensure a good physical stability. Differential scanning calorimetry (DSC), transmission electron microscopy (TEM), and scanning electron microscopy (SEM) studies suggested that triclosan was molecularly dispersed in the nanoparticle batches containing up to 31% of triclosan, with good encapsulation efficiency (95.9%). The results of the *in vitro* permeation studies showed the following order for the permeability coefficients: Solution > cream ≈ nanoparticles; while for the amount retained in the skin, the order was as follows: cream > nanoparticles ≈ solution. Nanoparticles, being free of surfactants or other potentially irritant agents, can be a good option for the delivery of triclosan to the skin, representing a good alternative for the treatment of acne.

1. Introduction

The cutaneous route offers diverse advantages as a site for drug administration. However, due to the natural properties of the skin as a protection barrier, the search for new strategies able to enhance the penetration of drugs has become essential [1]. On the one hand, different carrier systems have been proposed in an attempt to favor the transport of drugs through the skin, enabling drug retention and in some cases allowing a controlled release [2–5]. Among these systems, polymeric nanoparticles are expected to be able to form a depot in the hair follicles, providing a targeted controlled drug delivery [6]. On the other hand, penetration enhancers are commonly used to improve drug absorption [7–11]. Surfactants and bile salts are among the most commonly studied enhancers for cutaneous administration. Typically, both cationic and anionic surfactants are more potent enhancers than their nonionic counterparts, but they are also more toxic [12–14].

Acne is a common disorder experienced by up to 80% of individuals between 11 and 30 years of age, and by up to 5% of older adults [15]. It is a common multifactorial disorder of the pilosebaceous follicles, involving sebaceous hyperplasia, follicular hyperkeratinization, hormone imbalance, bacterial infection, immune hypersensitivity; and, in some cases, there is evidence of genetic influence [16–21]. Since microbial colonization is a factor for the development of acne, triclosan was used in our study due to its strong antimicrobial activity against *Propionibacterium acnes* [2,22]. A variety of commercial formulations containing triclosan are available in the market to treat acne. Although, in this study, triclosan-loaded nanoparticles are proposed as a new formulation for the treatment of acne, it is clear that applications are not limited to this skin complaint. In a previous work, our group reported the preparation and characterization of triclosan nanoparticles for periodontal treatment [23].

In the present work, nanoparticles were prepared through the emulsification–diffusion by solvent displacement process and were characterized by their size, Zeta potential, encapsulation efficiency, and morphology. *In vitro* percutaneous permeation through pig ear skin was evaluated for triclosan-loaded nanoparticles and was compared with that obtained with two formulations available in the market for the treatment of acne: An o/w emulsion and a solution.

* Corresponding author. División de Estudios de Posgrado (Laboratorio de Posgrado en Tecnología Farmacéutica), Facultad de Estudios Superiores Cuautitlán, UNAM. Av. 1° de Mayo s/n, Campo 1, Cuautitlán Izcalli, C.P. 54704, Estado de México, Mexico. Tel.: +52 55 56232065; fax: +52 55 58938675.
E-mail address: ganemq@hotmail.com (A. Ganem).

0939-6411/$ - see front matter © 2011 Elsevier B.V. All rights reserved.
doi:10.1016/j.ejpb.2011.01.017

2. Materials and methods

2.1. Materials

Triclosan (M.W. 289.5) was a contribution from Multiquim (Mexico D.F.), Eudragit® E 100 was provided by Helm (Mexico), poly (vinyl alcohol) (Mowiol® 4-88) was purchased from Glomarza, Mexico, and was used as stabilizer. Monobasic potassium phosphate, methyl ethyl ketone, ethanol, and methanol were obtained from Fermont (Productos Químicos Monterrey, Mexico). Brij® 58 was provided by Canamex, S.A., Mexico; hydrochloric acid and sodium hydroxide were obtained from J.T. Baker, USA. All other chemicals were of analytical grade and were used without further purification. Water was obtained from a Milli-Q System (Millipore, Schwalbach, Germany). Porcine ear skin was obtained from the slaughterhouse immediately after pig's death.

2.2. Nanoparticle preparation

Nanoparticles were prepared using the emulsification–diffusion by solvent displacement method [24]. The organic solvent (methyl ethyl ketone) and water were mutually saturated in order to ensure the initial thermodynamic equilibrium of both liquids. Following separation of the two phases, the polymer (Eudragit® E 100) and triclosan were dissolved in the water-saturated organic solvent, and this solution was emulsified with a solvent-saturated aqueous solution containing 5% (w/v) of poly (vinyl alcohol). Emulsification was performed using a stirrer (Caframo® RZR-1, Germany) at 2000 rpm for 10 min. Finally, the organic solvent was removed by vacuum steam distillation, in order to promote the diffusion of the solvent from the internal to the external phase and induce polymer aggregation to obtain nanoparticles. All dispersions were centrifuged using an Optima® LE-80 K ultracentrifuge (Beckman, USA), and nanoparticles were resuspended by magnetic stirring and sonication.

The effect of temperature (30, 60 and 90 °C) and solvent elimination rate (30, 90 and 150 rpm) during vacuum steam distillation on particle size was evaluated for unloaded nanoparticles. According to the results obtained, no significant differences in size were observed (Fig. 1). Hence, the temperature and rate of solvent elimination chosen were 30 °C and 30 rpm, respectively, due to the feasibility of the method. Some batches were lyophilized for 36 h using a freeze-drier (Labconco®, USA). The resulting nanoparticles were then stored in a dessicator until used. Batches with increasing amounts of triclosan (up to 60% with respect to polymer weight) were prepared in order to determine the maximum entrapped amount. Table 1 shows the amounts of triclosan used in each batch.

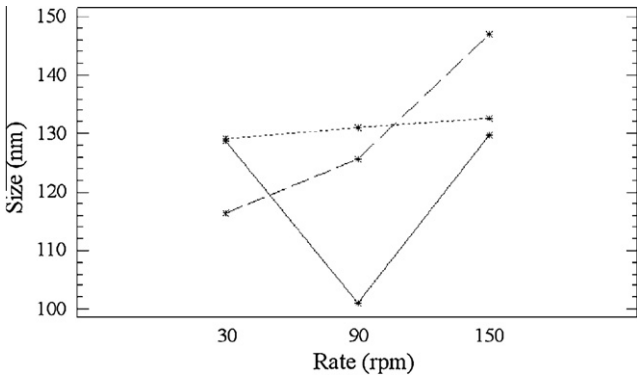

Fig. 1. Influence of solvent elimination rate (rpm) and temperature during the vacuum steam distillation, on nanoparticle size 30 °C (——); 45 °C (–); and 60 °C (· · · · · ·), $P > 0.5$..

Table 1
Composition of nanoparticle batches with increasing amounts of triclosan, prepared in order to determine the maximum entrapped amount.

Batch	Eudragit® E 100 (mg)	Eudragit® E 100 (% w/w)	Triclosan (mg)	Triclosan (% w/w)
1	400	100.00	0	0.00
2	400	95.24	20	4.76
3	400	90.91	40	9.09
4	400	86.96	60	13.04
5	400	83.33	80	16.67
6	400	80.00	100	20.00
7	400	74.07	140	25.93
8	400	68.97	180	31.03
9	400	64.52	220	35.48
10	400	60.61	260	39.39
11	400	57.14	300	42.86
12	400	54.05	340	45.95
13	400	51.28	380	48.72
14	400	48.78	420	51.22
15	400	46.51	460	53.49
16	400	44.44	500	55.56
17	400	40.00	600	60.00

2.3. Particle size analysis

Nanoparticles average size, polydispersity index, and particle size distribution were determined by photon correlation spectroscopy, using a Nanosizer® Coulter N4 Plus (Beckman, USA). Dispersions were diluted with distilled water to ensure that the light scattering signal was within the sensitivity range of the instrument. Measurements were made in triplicate for all batches prepared and were performed at a 90° scattering angle at 25 °C ($n = 3$).

2.4. Differential scanning calorimetry (DSC)

Samples of either ≈4 mg of drug, polymer, stabilizer, or both loaded and unloaded batches (previously freeze-dried) were weighed directly in standard aluminum pans. Studies were carried out at a constant heating rate of 10 °C/min and scanned from 0 to 300 °C, under constant purging of nitrogen at 50 ml/min, using a DSC Q 10 (TA Instruments, USA). Indium was used as the standard reference material to calibrate the DSC instrument.

2.5. Superficial charge

The Zeta potential of nanoparticle batches containing different amounts of triclosan was determined using a Zetasizer, Malvern Systems (ZEN 3600, United States), at the viscosity and dielectric constant of water, with an electrical current of 150 V at 25 °C. Deionized water was used as dispersion medium. Electrophoretic mobility was converted into Zeta potential by the Helmholtz–Smoluchowski equation ($n = 3$).

2.6. Encapsulation efficiency

The 'encapsulation efficiency' parameter refers to the percentage of drug entrapped with respect to the total amount of drug added through the nanoparticle preparation process. Freeze-dried samples of loaded and placebo nanoparticles were dissolved in ethanol, and suitable dilutions were performed until achieving an acceptable triclosan concentration. Quantification was performed by spectrophotometry at 285 nm ($n = 3$), using an UV–Vis spectrophotometer (Varian, Cary 50, Australia). The triclosan content in nanoparticles was expressed as the ratio of the amount of triclosan found in nanoparticles and the total initial amount of triclosan used in the preparation of the batch, and was represented as a percentage, according to the following expression:

$$\%\ \text{Encapsulation efficiency} = \frac{\text{Amount of triclosan found in nanoparticles}}{\text{Total initial amount of triclosan}} \times 100 \quad (1)$$

2.7. Morphology studies

The morphological examination of nanoparticles was performed by scanning electron microscopy (SEM) using a JSM-6400 scanning electron microscope (JEOL, Tokyo, Japan). A concentrated aqueous dispersion of nanoparticles was finely spread over stubs and dried under vacuum. The sample was coated with a thick gold layer of ~20 nm (1200 V, 5 mA and 0.15 Torr for 6 min). The morphology of nanoparticulate systems, such as shape and occurrence of aggregation phenomena, was also characterized by transmission electron microscopy (TEM) using a transmission electron microscope (JEOL 2010, Tokio, Japan). Samples were diluted with distilled water as dispersion medium and were placed on copper grids for viewing, with a voltage of 200 kV and at a resolution of 1.9 A (40,000 X).

2.8. Skin tissue

Full-thickness porcine ear skin was recovered from the slaughterhouse, following the slaughter of the animals and before being treated with vapor or hot water. The subcutaneous fat was removed from the skin, and the tissue was cut with a dermatome (Zimmer, Mod. 901, USA) to obtain a skin thickness ranging from 650 to 750 μm. Finally, the resulting skin was stored frozen at −35 °C before use.

2.9. In vitro permeation kinetics

In vitro permeation studies ($n = 6$) were carried out placing the skin (0.63 cm^2) between the donor and receptor compartments of vertical Franz-type glass diffusion cells. Two milliliters of the receptor phase (phosphate buffer pH 7.4 with addition of 3% w/v of Brij® 58 to keep *sink* conditions) were constantly stirred with a Teflon-coated magnetic bar and maintained at 37 °C. The donor phase was filled with 0.5 ml of formulation (nanoparticles, solution, or emulsion o/w). At selected time intervals, the receptor medium was collected and replaced with fresh medium. Samples were analyzed spectrophotometrically at 285 nm. Triclosan concentrations were obtained using a suitable calibration curve, correcting for the dilution effect.

At the end of the experiments, triclosan was extracted from the skin by soaking the tissues in ethanol for 21 h at room temperature. Triclosan content was analyzed by spectrophotometry at 285 nm. At least six measurements of each sample were conducted.

2.10. Statistical analysis

The size and charge of nanoparticles, the permeability coefficients, and the amount of triclosan extracted from the skin were statistically evaluated by one-way analysis of variance (ANOVA). Post hoc comparisons of individual group means were performed with the Duncan test. Differences were considered significant if $P < 0.05$.

3. Results and discussion

In this study, nanoparticles were prepared using the emulsification–diffusion by solvent displacement method. Eudragit® E 100 was chosen as the polymeric material due to its dissolution properties (i.e., soluble in acid media up to pH 5, swellable and permeable above pH 5). Taking into account the skin pH, release from nanoparticles is expected to occur by dissolution of the polymer and/or by diffusion through the polymeric matrix. The effect of temperature and solvent elimination rate during vacuum steam distillation on particle size was evaluated in unloaded nanoparticles. As shown in Fig. 1, no significant differences in size were observed. A clear relationship between the size of triclosan-loaded nanoparticles and the amount of triclosan for the different batches was not found. As shown in Fig. 2, nanoparticle size ranged from 120 to 240 nm. Although for batches 1–7 (0–140 mg of triclosan) the size apparently increased linearly, unexpectedly, batches 8–17 containing a greater amount (180–600 mg of triclosan) showed a smaller size. The Zeta potential for batches 1–11 was positive due to the cationic charge of the Eudragit® E 100 polymer and was high enough (20–39 mV) to provide a stable suspension of particles (Fig. 3). Usually, the Zeta potential required must be $|Z| > 30$–50 to ensure an acceptable physical stability by a good electrostatic repulsion [25]. A greater amount of triclosan in nanoparticles (batches 12–17) resulted in a lower Zeta potential that, as mentioned, can be associated with a lower stability.

Differential scanning calorimetry (DSC) was used to characterize the thermal behavior of molecules by studying phase transitions. Shifts of exothermic and endothermic peaks are usually related to interactions between drugs and polymers [26].

Thermograms for the materials involved in nanoparticles preparation (stabilizer, polymer, and drug), as well as for a drug–polymer physical mixture (50:50%), are shown in Fig. 4. As can be observed, the stabilizer (a) shows an endotherm near 200 °C, related to the melting point of poly (vinyl alcohol) [27]. The value of T_g for Eudragit® E 100 is found near 54 °C (b); therefore, as expected, unloaded nanoparticles (c) show solely the endotherm related to the polymer's T_g. Triclosan (e) shows an endothermic peak at 54 °C, associated with its melting point (melting point 54–57 °C, [28]). In the case of the physical mixture (d), the drug melting point is clearly observed, indicating no association between the drug and the polymer. The polymer's T_g and the drug melting point are very close; however, the presence of triclosan is clearly evident by a sharp well-defined peak. Batches 2–6 of loaded nanoparticles (20–100 mg of triclosan) show endotherms related to T_g, but they are not associated with triclosan melting point, indicating that triclosan was molecularly dispersed into the polymeric matrix (data not shown).

The thermograms of some triclosan-loaded nanoparticle batches (7, 8, 11 and 16) are shown in Fig. 5. No melting point was observed for triclosan entrapped in nanoparticles, presenting only the endothermic peak associated with the glass transition temperature of the polymer. This implies a close interaction between the polymer and the drug, suggesting a molecular dispersion

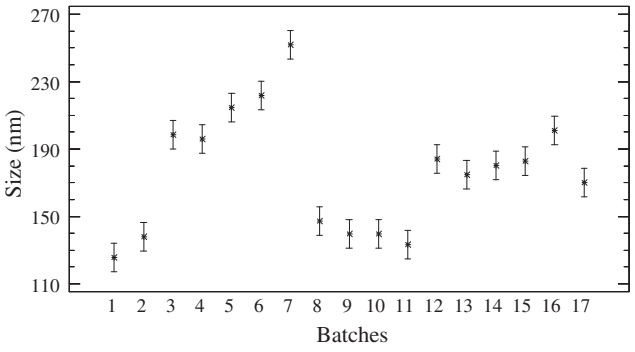

Fig. 2. Particle size for nanoparticle batches with increasing amounts of triclosan (from 0% to 60%).

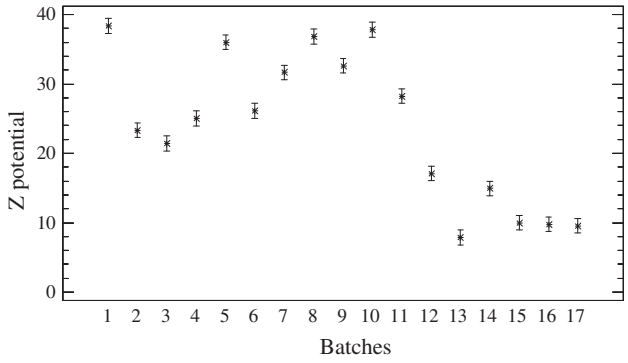

Fig. 3. Zeta potential for nanoparticle batches with increasing amounts of triclosan.

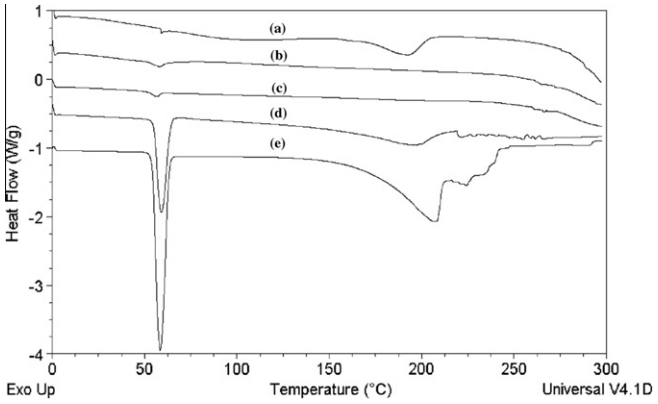

Fig. 4. Thermograms for stabilizer [poly (vinyl alcohol)] (a); polymer [Eudragit® E 100] (b); unloaded nanoparticles [0% triclosan] (c); a physical mixture of triclosan and Eudragit® E 100 (d); and triclosan (e).

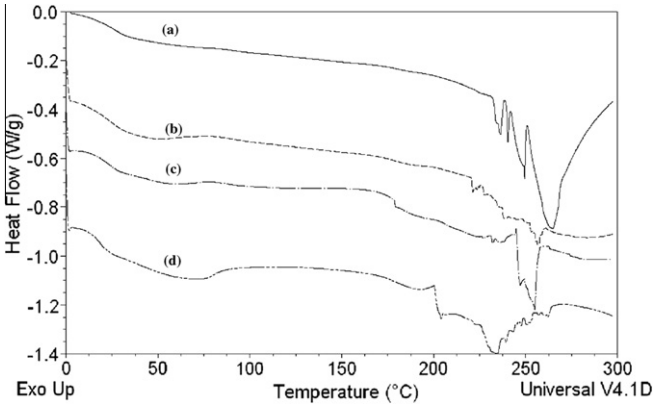

Fig. 5. Thermograms for batches with increasing amounts of triclosan: (a) batch 7, 25.93%; (b) batch 8, 31.03%; (c) batch 11, 42.86%; (d) batch 16, 55.56%.

of drug into the polymer matrix. It is important to mention that the T_g of Eudragit® E 100 shifts to lower temperatures as the amount of triclosan increases. This behavior can be attributed to a loss of polymer crystallinity and to the fact that triclosan can behave as a nonconventional plasticizer, favoring film formation. Similar results have been reported by other researchers [2,23]. Comparing the thermograms of unloaded nanoparticles (Fig. 4) with those containing triclosan (Fig. 5), an endothermic event is observed at temperature above 200 °C, probably related to triclosan decomposition. As the content of triclosan increased in the nanoparticles, this endothermic behavior shifted to a lower temperature and it became more evident.

Morphology studies using SEM show that loaded nanoparticles (Fig. 6 a) have a spherical shape and a solid surface, and that particle size agrees with that determined by photon correlation spectroscopy. However, visualization by this technique was difficult due to the tendency of Eudragit® E 100 to form films. This was the reason for using TEM. Similar results regarding size were obtained by TEM (Fig. 6b and c), showing nanoparticles of less than 200 nm. Nevertheless, as shown in Fig. 6c, a high particle concentration results in nanoparticle fusion and film formation.

DSC, TEM, and SEM studies (Figs. 5 and 6) confirm that triclosan is molecularly dispersed in nanoparticle batches containing up to 31% and that above this ratio, triclosan interacts with the polymer, suggesting that it acts as a nonconventional plasticizer, promoting the fusion of the nanoparticle.

According to these results, batch 8, containing 31% of triclosan, was chosen for *in vitro* permeation studies, due to its high encapsulation efficiency (95.9%) and good stability. Nanoparticles used for permeation studies had an average particle size of 147 ± 37 nm. Permeation studies were performed over eight hours. Two slopes were observed during permeation, and therefore, two fluxes and two permeability coefficients (C_p) are reported in Table 2. Since the amount of triclosan was different for the commercial formulations and nanoparticles (a fact that affects permeation capability), a ratio of the total amount permeated or the amount retained in the skin with respect to the triclosan concentration in each formulation was calculated. As shown in Table 2, and in Figs. 7 and 8, the highest total amount permeated (PA) was obtained for the solution, while the greatest amount retained in the skin (RA) was found for the emulsion.

In the case of the solution and the emulsion, the high triclosan permeability can be attributed to its high surfactant content. Surfactants are incorporated into many therapeutic and cosmetic preparations. Usually, they are added to formulations in order to stabilize emulsions and suspensions or to solubilize lipophilic active ingredients. Surfactants have been shown to influence skin permeability in a number of ways. Many surfactants penetrate into the skin and act directly on skin components, sometimes inducing a loss of membrane integrity, e.g., by lipid or protein extraction or by protein denaturation [12,14]. Sodium lauryl sulfate and sodium laureth sulfate are anionic surfactants; lauryl glucoside and steareth 20 are other surfactants used as emulsifier agents. They are contained in the commercial formulations for the treatment of acne tested in this study. Structural parameters, such as chain length, the degree and position of insaturations, and the nature of substituents in the molecule, can influence their action as skin penetration enhancers. It is well accepted that the linear alkyl chain of 12 carbon atoms maximizes the effect of a surfactant on membrane permeability. The C_{12} chain has an oil/water intermediate solubility and is able to penetrate the lipid bilayer [12,14,29]. Among a series of polyoxyethers, lauryl (C_{12}) ether was reported to be the most effective enhancer for ibuprofen, followed by oleyl (C_{18}) ether [7]. So, these surfactants had the potential to fluidize lipids within the stratum corneum and to improve drug permeation into the skin. However, this potential enhancing effect is often directly proportional to the degree of skin irritation [14].

Sodium lauryl sulfate and sodium laureth sulfate have been classified as irritants, and lauryl glucoside has been classified as slightly irritant [13,14,30]. In general, surfactants can cause major potential damage to the skin in patients with acne.

In addition to the enhancing effect of surfactants, the cream tested in this work contains a dermoabrasive cleaner with aluminum oxide particles, which can also contribute to triclosan penetration (Table 2 and Fig. 8). On the other hand, the fatty

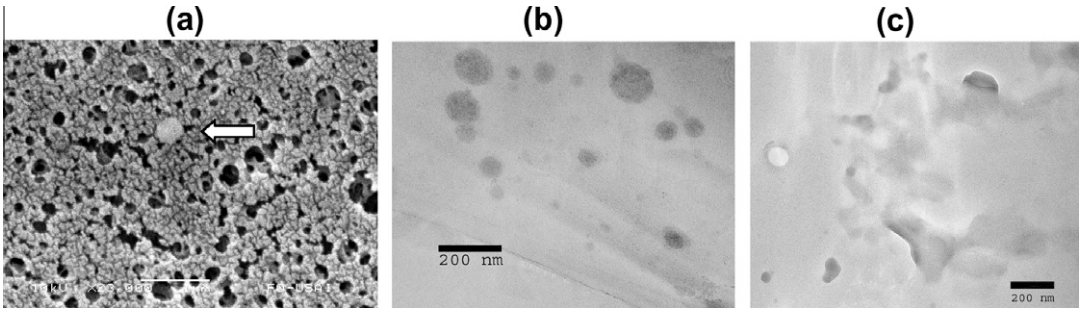

Fig. 6. Micrographs for batch 8 (31.03% of triclosan): (a) SEM (bar = 1 μm); (b and c) TEM (bar = 200 nm).

Table 2
Permeation parameters for the three formulations PA = Total permeated amount/vehicle concentration; RA = Drug retained in the skin/vehicle concentration.

		Solution	Emulsion (w/o)	Nanoparticle dispersion
Flux (μg/cm^2 h)	0–2 h	6.2765 ± 3.29	6.3457 ± 1.37	10.6675 ± 5.13
	2–8 h	4.8371 ± 1.59	4.0942 ± 1.17	2.0611 ± 0.92
C_p (μm/h)	0–2 h	24.0845 ± 12.62	6.0697 ± 1.31	5.9264 ± 2.85
	2–8 h	18.5611 ± 6.11	3.9161 ± 1.12	1.1451 ± 0.51
PA		13.7252 ± 3.97	3.5795 ± 0.87	2.0623 ± 0.96
RA		2.3145 ± 1.45	6.5568 ± 0.96	1.5923 ± 0.40

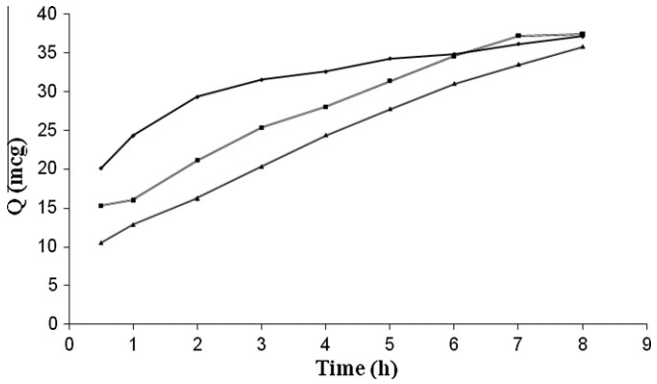

Fig. 7. Permeation kinetics of triclosan from three formulations using pig ear skin (n = 6). (♦) Nanoparticle dispersion (n = 5); (■) emulsion (n = 6); (▲) solution (n = 9).

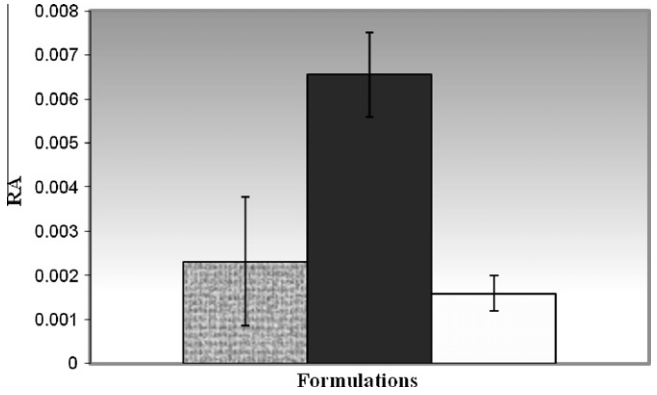

Fig. 8. Triclosan retained in pig ear skin at the end of the permeation experiments. (▒) Solution (n = 6); (■) emulsion (n = 4); (□) nanoparticle dispersion (n = 6). RA = Retained amount/concentration.

components of the emulsion favored the penetration and accumulation of triclosan in the skin, obtaining the highest RA, due to the great affinity of these kinds of components for cutaneous lipid domains. The ANOVA test showed no differences for the total permeated amount (PA) between the emulsion and nanoparticles, nor for the amount retained in the skin (RA) between the solution and nanoparticles ($P > 0.5$).

It is important to point out that for all formulations, the permeation profiles showed an apparent *burst* effect (Fig. 7). The flux of triclosan was fivefold higher for nanoparticles than for the solution or the emulsion during the first two hours. This suggests that nanoparticles can penetrate quickly into hair follicles, and then saturate this way, gradually decreasing drug flux. The solution and the emulsion had practically constant fluxes throughout the permeation experiment.

Therefore, nanoparticle suspension can be potentially effective in the treatment of acne, due to the small size of nanoparticles that allows a target site (mainly in the hair follicle) and could form a depot to control the delivery of triclosan. In this respect, previous reports have revealed, through surface images, that (i) polystyrene nanoparticles accumulated preferentially in the follicular openings, (ii) this distribution increased in a time-dependent manner, and (iii) follicular localization was favored by the smaller particle size [6]. This is a good point for nanoparticles, since they can accumulate in the target site, releasing triclosan directly in the affected site. Furthermore, this formulation lacks enhancing agents that could cause some irritant reaction, contrary to the two commercial formulations.

4. Conclusions

In this study, Eudragit® E 100 nanoparticles were prepared using the emulsification–diffusion by solvent displacement method. All batches showed a size below 300 nm. DSC, TEM, and SEM studies confirm that triclosan is molecularly dispersed in nanoparticle batches containing up to 31% triclosan, with high encapsulation efficiency (95.9%) and a good stability. At higher drug content, triclosan interacts with the polymer, with a decrease in its glass transition temperature, acting as a nonconventional plasticizer, and then promoting the fusion of the nanoparticles. According to permeation results (taking into account the concentration of triclosan in each formulation), the following order was found (i) for

the amount permeated: solution > emulsion ≈ nanoparticles; (ii) for the amount retained in the skin: emulsion > solution ≈ nanoparticles. It is expected that the colloidal properties of nanoparticles will favor penetration through hair follicles, where they can form a depot, promoting triclosan release from these sites. Further studies should be conducted in this sense.

Acknowledgment

The authors acknowledge a grant from CONACyT (Ref. 81883) and PAPIIT (Ref. IN209709). The authors are grateful to Mr. Rodolfo Robles for his technical assistance with the SEM images.

References

[1] G. Cevc, Drug delivery across the skin, Exp. Opin. Invest. Drugs. 6 (12) (1997) 1887–1937.
[2] J.-C. Kim, M.-E. Song, M.-J. Kim, E.-J. Lee, S.-K. Park, M.-J. Rang, H.-J. Ahn, Preparation and characterization of triclosan-containing vesicles, Colloid Surface B 26 (2002) 235–241.
[3] R.H. Müller, M. Radtke, S.A. Wissing, Solid lipid nanoparticles (SLN) and nanostructured lipid carriers (NLC) in cosmetic and dermatological preparations, Adv. Drug. Deliv. Rev. 54 (2002) S131–S155.
[4] G. Cevc, Lipid vesicles and other colloids as drug carriers on the skin, Adv. Drug. Deliv. Rev. 56 (2004) 675–711.
[5] F. Maestrelli, M. Garcia-Fuentes, P. Mura, M.J. Alonso, A new drug nanocarrier consisting of chitosan and hydoxypropylcyclodextrin, Eur. J. Pharm. Biopharm. 63 (2006) 79–86.
[6] R. Alvarez-Román, A. Naik, Y.N. Kalia, R.H. Guy, H. Fessi, Skin penetration and distribution of polymeric nanoparticles, J. Control. Release 99 (2004) 53–62.
[7] E.-S. Park, S.-Y. Chang, M. Hahn, S.-Ch. Chi, Enhancing effect of polyoxyethylene alkyl ethers on the skin permeation of ibuprofen, Int. J. Pharm. 209 (2000) 109–119.
[8] J. Cázares-Delgadillo, A. Naik, Y.N. Kalia, D. Quintanar-Guerrero, A. Ganem-Quintanar, Skin permeation enhancement by sucrose esters: a pH-dependent phenomenon, Int. J. Pharm. 297 (2005) 204–212.
[9] J.J. Escobar-Chávez, Estudio de la penetración a través de la piel de naproxeno sódico utilizando agentes promotores de penetración (Azona® y Transcutol®), y de digluconato de clorhexidina mediante iontoforesis, Ph.D. Thesis, Facultad de Química, UNAM, Mexico, 2006, pp. 10–22.
[10] A. Choi, H. Gang, I. Chun, H. Gwak, The effects of fatty acids in propylene glycol on the percutaneous absorption of alendronate across the excised hairless mouse skin, Int. J. Pharm. 357 (2008) 126–131.
[11] K. Vávrová, K. Lorencová, J. Klimentová, J. Novotný, A. Holý, A. Hrabálek, Transdermal and dermal delivery of adefovir: effects of pH and permeation enhancers, Eur. J. Pharm. Biopharm. 69 (2008) 597–604.
[12] H.A. Ayala-Bravo, D. Quintanar-Guerrero, A. Naik, Y.N. Kalia, J.M. Cornejo-Bravo, A. Ganem-Quintanar, Effects of sucrose oleate and sucrose laureate on in vivo human stratum corneum permeability, Pharmaceut. Res. 20 (2003) 1267–1273.
[13] A. Mehling, M. Kleber, H. Hensen, Comparative studies on the ocular and dermal irritation potential of surfactants, Food. Chem. Toxicol. 45 (2007) 747–758.
[14] E. Touitou, B.W. Barry, Enhancement in Drug Delivery, CRC Press, Taylor & Francis Group, United States of América, 2007. pp. 233–251.
[15] V. Goulden, G.I. Stables, W.J. Cunliffe, Prevalence of facial acne in adults, J. Am. Acad. Dermatol. 41 (1999) 577–580.
[16] G.M. White, Recent findings in the epidemiologic evidence, classification, and subtypes of acne vulgaris, J. Am. Acad. Dermatol. 39 (1998) S34–S37.
[17] V. Bataille, H. Snieder, A.J. MacGregor, P. Sasieni, T.D. Spector, The influence of genetics and environmental factors in the pathogenesis of Acne: a Twin Study of Acne in Women, J. Invest. Dermatol. 119 (6) (2002) 1317–1322.
[18] H. Gollnick, Current concepts of the pathogenesis of acne: implications for drug treatment, Drugs 63 (2003) 1579–1596.
[19] U. Jappe, Pathological mechanisms of acne with special emphasis on Propionibacterium acnes and related therapy, Acta Derm. Venereol. 83 (2003) 241–248.
[20] I. Nagy, A. Pivarcsi, K. Kis, A. Koreck, L. Bodai, A. McDowell, H. Seltmann, S. Patrick, C.C. Zouboulis, L. Kemény, Propionibacterium acnes and lipopolysaccharide induce the expression of antimicrobial peptides and proinflammatory cytokines/chemokines in human sebocytes, Microbes Infect. 8 (2006) 2195–2205.
[21] C.G. Burkhart, C.N. Burkhart, Expanding the microcomedone theory and acne therapeutics: propionibacterium acnes biofilm produces biological glue that holds corneocytes together to form plug, J. Am. Acad. Dermatol. 57 (2007) 722–724.
[22] T.-W. Lee, J.-Ch. Kim, S.-J. Hwang, Hydrogel patches containing Triclosan for acne treatment, Eur. J. Pharm. Biopharm. 56 (2003) 407–412.
[23] E. Piñon-Segundo, A. Ganem-Quintanar, V. Alonso-Pérez, D. Quintanar-Guerrero, Preparation and characterization of triclosan nanoparticles for periodontal treatment, Int. J. Pharm. 294 (2005) 217–232.
[24] D. Quintanar-Guerrero, E. Allémann, H. Fessi, E. Doelker, Pseudolatex preparation using a novel emulsion–diffusion process involving direct displacement of partially water-miscible solvents by distillation, Int. J. Pharm. 188 (1999) 155–164.
[25] Dispersion Technology Systems, Nanometric group, Malvern Instrument., Inc., South Borough, MA, May 2005.
[26] B. Sarmento, D. Ferreira, F. Veiga, A. Ribeiro, Characterization of insulin-loaded alginate nanoparticles produced by ionotropic pre-gelation through DSC and FTIR studies, Carbohyd. Polym. 66 (2006) 1–7.
[27] R.C. Rowe, P.J. Sheskey, S.C. Owen, Pharmaceutical Excipients, Electronic Version. Ed. Pharmaceutical Press and American Pharmacists Association, 2004.
[28] A.C. Moffat, Clarke's Isolation and Identification of Drugs, second ed., The Pharmaceutical Press, London, 2004.
[29] R.A. Tupker, J. Pinnagoda, J.P. Nater, The transient and cumulative effect of sodium lauryl sulphate on the epidermal barrier assessed by transepidermal water loss: inter-individual variation, Acta Derm. Venereol. (Stockh) 70 (1990) 1.
[30] T.J. Hall-Manning, G.H. Holland, G. Rennie, P. Revell, J. Hines, M.D. Barratt, D.A. Basketter, Skin irritation potential of mixed surfactant systems, Food Chem. Toxicol. 36 (1998) 233–238.